Eur. J. Mineral.
2007, **19**, 671–680
Published online October 2007

This paper was presented at the EMPG XI symposium in Bristol, U.K. (September 2006)

The effect of CO_2 on the solubility of H_2O-Cl fluids in andesitic melt

ROMAN E. BOTCHARNIKOV*, FRANCOIS HOLTZ and HARALD BEHRENS

Institut für Mineralogie, Universität Hannover, Callinstr. 3, 30167, Hannover, Germany
*Corresponding author, e-mail: R.Botcharnikov@mineralogie.uni-hannover.de

Abstract: The solubility of C-O-H-Cl-bearing fluids in andesitic melt was investigated experimentally at temperatures of 1050 and 1200 °C and pressure of 200 MPa. The CO_2-free andesitic melts produced experimentally contained up to 5.5–6 wt.% H_2O and up to 2.5 wt.% Cl at the investigated conditions. The complex non-linear relationship between the concentrations of H_2O and Cl in the melt indicates a strong non-ideality of the H_2O-salt-bearing fluid phase(s), presumably resulting in the formation of two immiscible fluids. The addition of CO_2 to the system (80–800 ppm dissolved CO_2 in the melt) has two effects: a simple dilution of the fluid at low bulk Cl concentration and a significant influence on the mixing properties of the H_2O- and Cl-bearing fluids related to the enlargement of the immiscibility gap in the fluid at higher bulk Cl content. The first effect results in lower H_2O (by ~ 1 wt.%) and almost constant Cl concentrations in the melt, while the second effect causes an increase in activity coefficients of both H_2O and Cl. This effect of CO_2 is expected to be most pronounced at low pressures and high CO_2 concentrations in Cl-bearing mafic melts due to an enlargement of the immiscibility gap in fluids with decreasing pressure and an increase in proportions of divalent cations.

Key-words: andesite, silicate melt, solubility, H_2O, CO_2, Cl, C-O-H-Cl fluids, speciation, immiscibility.

1. Introduction

A release of volatiles from magmas is commonly a driving force for magma ascent from crustal depths and for magmatic eruptions. The kinetics and efficiency of degassing processes are controlled by several parameters like pressure, temperature, silicate melt composition, and activity of dissolved volatile components. Natural subduction-related magmas contain a wide range of volatiles with significant proportions of H_2O and CO_2, *e.g.* glass inclusions, preserved in phenocrysts, contain up to 6–8 wt% H_2O and 2500–3000 ppm CO_2 (Sisson & Grove, 1993; Wallace, 2005). Volcanic gases of typical subduction-related volcanoes have also predominant abundances of H_2O and CO_2 with concentrations varying from ~ 80 to 99 mole% and from < 1 to ~ 8 mole %, respectively (*e.g.*, Symonds *et al.*, 1994). Hence, the measured concentrations of H_2O and CO_2 in melt inclusions and volcanic gasses are commonly used to estimate magma storage conditions and magma evolution based on the empirical and semi-empirical models (*e.g.*, Dixon *et al.*, 1995; Papale, 1999; Tamic *et al.*, 2001; Newman & Lowenstern, 2002; Behrens *et al.*, 2004a; Liu *et al.*, 2005; Papale *et al.*, 2006).

However, other volatiles like S and Cl have also a wide range of concentrations in arc magmas and volcanic gases. For instance, arc magmas may contain from 50 to 2000 ppm S and from 500 to 2500 ppm Cl whereas concentrations of S and Cl in the gases may reach up to 50 mole% SO_2+H_2S and up to 6 mole% HCl (*e.g.*, Symonds *et al.*, 1994; Wallace, 2005). Moreover, these volatile components play an important and critical role in the fluid saturation, volatile release and degassing of natural magmas, thus models, predicting fluid saturation based on H_2O and CO_2 only, may be not completely correct. The importance of mixed fluids in magma degassing and crystallization processes was emphasized in several experimental studies (*e.g.*, Webster & Holloway, 1988; Botcharnikov *et al.*, 2004; Webster *et al.*, 2004; Mathez & Webster, 2005) and models (*e.g.*, Moretti *et al.*, 2003; Moretti & Papale, 2004; Scaillet & Pichavant, 2003; 2005). These works indicate complex relationships between concentrations and partitioning of volatiles between silicate melts and coexisting fluids, resulting in sometimes poorly predictable behavior. In this study we present a new attempt to better understand such a complex behavior of mixed fluids in natural magmatic systems. For the experiments we have choosen an andesitic composition which is typical for subduction-related volcanism (*e.g.*, Gill, 1981). We report new experimental data on the solubility of C-O-H-Cl fluids in andesitic melts at 200 MPa.

2. Experimental methods

2.1. Starting material

The starting material was a synthetic analogue of an andesitic melt (Table 1), corresponding to the andesitic com-

DOI: 10.1127/0935-1221/2007/0019-1752

0935-1221/07/0019-1752 $ 4.50

Table 1. Starting composition of synthetic andesite (normalized to 100 %). A/CNK is a molar ratio of Al_2O_3 / ($CaO + Na_2O + K_2O$) in the melt.

	Andesite
SiO_2	57.44
TiO_2	1.06
Al_2O_3	17.53
FeO^{tot}	7.20
MnO	0.12
MgO	4.31
CaO	7.42
Na_2O	3.32
K_2O	1.61
Total	100.00
A/CNK	0.850

positions from Unzen volcano, Japan (*e.g.*, Nakada & Motomura, 1999; Holtz *et al.*, 2005). It was prepared from a mixture of oxides (SiO_2, TiO_2, Al_2O_3, Fe_2O_3, MnO, MgO) and carbonates ($CaCO_3$, Na_2CO_3, K_2CO_3). The preparation of the starting glass is described in detail in (Botcharnikov *et al.*, 2006, in press).

2.2. Experimental strategy

Fifty mg of silicate glass powder (with a grain size < 200 μm) were loaded in 20 mm long (inner diameter of 2.6 mm) $Au_{80}Pd_{20}$ capsules. Five μl of aqueous HCl solution (0.9–33.5 wt% HCl) were added to the charge in the capsules. The initial concentrations of Cl in HCl solutions were verified using a Mettler DL25 Titrator (Table 2). In one experiment (ClC174), 1 μl of distilled H_2O and 15 mg of AgCl were charged into the capsule to increase the amount of bulk Cl in the system. Two experiments (Cl245 and ClC175) were nominally dry and contained only AgCl (~ 20 mg) as a Cl source. The amount of H_2O in the AgCl powder was negligable as detected by the Karl-Fischer titration (KFT) method. A special gas-loading device (Boettcher *et al*., 1989) was used to fill gaseous CO_2 into the capsule as described by (Botcharnikov *et al*., 2006). The amount of added CO_2 gas was in the range from 0.5 to 1.0 mg (see Table 2). Capsules were welded shut using a graphite arc welder. The mass proportions of the rock powder and fluid were quantified by measuring the weight gain after charging and welding (the measured values were corrected for the loss of noble metal on welding, *i.e.* we added 0.25 ± 0.10 mg to the final weight of the capsules as discussed by (Botcharnikov *et al*., 2006). In all our experiments the amounts of H_2O and Cl (+ CO_2) loaded into the capsules were sufficient to ensure fluid-saturation in andesitic melts at the investigated conditions.

Two different series of experiments, one with only H_2O- and Cl-bearing fluids and a second with H_2O-, Cl-, and CO_2-bearing fluids, were run at 200 MPa to investigate the effects of complex fluid composition on the solubility of volatiles in andesitic melt.

2.3. Experimental technique

The capsules were run in a vertically oriented internally heated pressure vessel (IHPV) at temperatures of 1200 °C and 1050 °C. Both temperatures correspond to superliquidus conditions for studied H_2O-rich andesite composition (*e.g.*, Botcharnikov *et al.*, in press). Water-poor experiments were conducted at 1200 °C, a temperature which is known to be above the liquidus at the employed pressure. Total pressure was measured and recorded continuously with an uncertainty of about 1 MPa using a strain gauge manometer. The variations of pressure during the experiments were ≤ 5 MPa. Temperature was measured with four unsheathed S-type ($Pt\text{-}Pt_{90}Rh_{10}$) thermocouples over a length of ~ 30 mm, and temperature variations were less than ± 5 °C. The IHPV was pressurized with Ar gas, and all experiments were performed at the intrinsic redox conditions of the vessel. At high temperature, the $Au_{80}Pd_{20}$ capsules were permeable to H_2 and, hence, hydrogen fugacity (fH_2) in the capsules was imposed by the IHPV. The oxygen fugacity (fO_2) within the capsules was controlled by the fugacity of water. In the capsules with H_2O-saturated melts (pure H_2O-fluid), fO_2 is close to that buffered by the $MnO\text{-}Mn_3O_4$ (MMO) assemblage or ~ 4 logarithmic units higher than the commonly-used quartz-fayalite-magnetite (QFM) buffer (verified by Berndt *et al.*, 2002 using the Ni-Pd redox sensor after Taylor *et al.*, 1992). With decreasing activity of H_2O in the system, the oxygen fugacity in the capsule also decreases. Using the mole fraction of H_2O in the fluid (see discussion below and Table 3), the lowest fO_2 in the nominally dry experiments was estimated to be about QFM+2. However, it must be noted that these estimations are based on the assumption that the activity of H_2O inside the capsules is proportional to the mole fraction of H_2O in the fluid phase (see *e.g.*, Botcharnikov *et al.*, 2005b). This assumption is probably not correct for the complex non-ideal H_2O-, Cl- and CO_2-bearing fluids and water activity is in fact higher than assumed. It would result in higher oxygen fugacity in the experiments.

The duration of the runs was 52–140 h. According to diffusivity data for water, Cl and carbon species in silicate melts at the studied conditions (*e.g.*, Behrens *et al.*, 2004c; Nowak *et al.*, 2004; Baker *et al.*, 2005), the applied run times were sufficient to allow equilibrium distribution of volatiles between fluid and andesitic melt, initially composed of a fine glass powder. The homogeneous distribution of the initial fluid phase within the pore space of fine-grained powder of glass is expected to enhance a fast reaction and equilibration of the silicate melt and the coexisting fluid. The samples were rapidly quenched (~ 150 °C/s) at the end of the run by dropping the capsules into the cold part of the vessel (Berndt *et al*., 2002).

3. Analytical methods

After the experiments all capsules were checked for possible leaks and only capsules from successful runs were used for further analyses. In most experiments, the

Table 2. The conditions and glass compositions of the 200 MPa experiments (1σ error).

Sample	T, °C	time h	HCl ini wt.%[a]	CO_2 ini [b], mg (±0.10)	n*	SiO_2	TiO_2	Al_2O_3	FeO^{tot}	MnO	MgO	CaO	Na_2O	K_2O	Cl	Total	H_2O melt, wt.% [d]	A/CNK
Cl130	1200	140	2.8	–	10	54.65 (33)	0.98 (6)	16.46 (26)	6.90 (48)	0.08 (10)	4.01 (22)	6.95 (25)	3.09 (17)	1.60 (5)	0.25 (1)	94.97	5.95 (10)	0.846
Cl131	1200	140	11.2	–	10	54.00 (58)	0.97 (6)	16.31 (12)	6.64 (28)	0.06 (11)	3.98 (13)	6.74 (35)	3.09 (15)	1.59 (8)	0.98 (2)	94.35	5.76 (10)	0.856
Cl239	1200	120	20.0	–	10	53.62 (56)	0.91 (8)	16.35 (24)	6.82 (30)	0.13 (7)	4.10 (14)	6.93 (30)	3.16 (25)	1.55 (12)	1.69 (2)	95.24	5.54 (8)	0.840
Cl240	1200	120	25.3	–	10	53.01 (24)	0.94 (5)	16.34 (27)	6.72 (47)	0.14 (8)	3.98 (18)	6.93 (27)	3.05 (28)	1.44 (9)	2.15 (2)	94.71	5.59 (13)	0.852
Cl243	1200	120	30.2	–	10	52.97 (27)	0.94 (5)	16.16 (31)	6.62 (50)	0.17 (10)	3.91 (19)	6.99 (13)	3.14 (41)	1.48 (11)	2.50 (1)	94.89	5.92 (11)	0.830
Cl245	1200	120	AgCl [c]	–	8	58.73 (26)	1.04 (5)	18.24 (30)	4.23 (31)	0.06 (5)	4.19 (18)	6.07 (34)	2.25 (21)	0.83 (8)	2.46 (2)	98.09	2.27 (11)	1.166
Cl84	1050	120	2.8	–	30	53.60 (26)	0.96 (3)	16.18 (13)	6.95 (20)	0.10 (3)	4.00 (8)	7.00 (16)	3.03 (16)	1.55 (5)	0.24 (1)	93.61	5.88 (10)	0.835
Cl85	1050	120	5.6	–	20	53.58 (20)	0.97 (4)	16.09 (12)	7.06 (32)	0.11 (4)	3.94 (8)	7.00 (14)	3.00 (12)	1.54 (8)	0.48 (1)	93.78	5.99 (10)	0.832
Cl86	1050	120	11.2	–	25	53.36 (24)	0.95 (4)	16.02 (15)	6.90 (27)	0.09 (5)	3.96 (7)	6.93 (12)	2.97 (14)	1.54 (5)	0.97 (1)	93.70	6.10 (10)	0.836
ClC148 *	1200	52	11.2	0.90	18	54.33 (52)	1.01 (7)	16.61 (27)	7.18 (36)	0.11 (12)	4.11 (12)	6.98 (27)	3.17 (26)	1.55 (11)	0.92 (3)	95.95	5.24 (13)	0.849
ClC149 *	1200	52	11.2	0.94	18	54.03 (48)	1.00 (7)	16.62 (27)	6.89 (49)	0.10 (11)	4.10 (12)	7.00 (18)	3.20 (29)	1.56 (13)	0.97 (3)	95.48	4.92 (10)	0.844
ClC150 *	1200	52	11.2	0.92	18	54.30 (69)	0.98 (8)	16.55 (24)	6.87 (50)	0.09 (12)	4.11 (17)	7.00 (28)	3.16 (32)	1.54 (10)	0.97 (3)	95.58	5.06 (8)	0.845
ClC151	1200	72	0.9	0.95	18	54.50 (43)	1.04 (6)	16.75 (30)	7.13 (44)	0.12 (6)	4.16 (18)	6.97 (30)	3.18 (24)	1.53 (11)	0.08 (1)	95.46	5.14 (10)	0.856
ClC152	1200	72	2.8	0.96	18	54.78 (49)	1.01 (8)	16.72 (30)	6.86 (49)	0.12 (12)	4.11 (22)	7.08 (30)	3.16 (23)	1.53 (10)	0.24 (1)	95.61	4.92 (11)	0.848
ClC153	1200	72	5.6	0.91	18	54.44 (46)	0.99 (5)	16.60 (31)	6.95 (40)	0.07 (12)	4.15 (16)	7.06 (31)	3.19 (37)	1.54 (8)	0.48 (2)	95.48	4.90 (9)	0.840
ClC154	1200	72	33.5	0.68	18	53.80 (47)	0.95 (7)	16.41 (30)	6.84 (35)	0.19 (9)	4.12 (18)	6.96 (20)	3.14 (35)	1.48 (11)	2.76 (6)	96.66	5.07 (6)	0.844
ClC171	1200	72	20.0	0.91	9	54.38 (51)	0.95 (5)	16.44 (23)	7.32 (17)	0.05 (8)	4.01 (17)	7.11 (28)	3.03 (23)	1.52 (6)	1.71 (1)	96.51	5.24 (9)	0.840
ClC172	1200	72	14.4	1.03	9	54.82 (22)	0.93 (4)	16.43 (20)	7.00 (22)	0.05 (9)	3.95 (13)	7.20 (28)	3.18 (17)	1.53 (7)	1.22 (1)	96.32	5.13 (10)	0.822
ClC173	1200	72	25.3	0.72	9	54.11 (46)	0.93 (6)	16.46 (23)	7.14 (59)	0.09 (4)	3.93 (15)	7.07 (22)	2.99 (19)	1.49 (13)	2.14 (3)	96.35	5.33 (10)	0.850
ClC174	1200	72	AgCl +H_2O [c]	0.54	9	57.64 (46)	1.01 (3)	17.25 (20)	5.62 (44)	0.02 (8)	4.04 (14)	6.70 (10)	2.31 (23)	1.04 (6)	2.64 (4)	98.27	3.57 (14)	1.009
ClC175	1200	72	AgCl [c]	0.70	8	59.96 (47)	0.98 (5)	18.21 (29)	4.27 (32)	0.04 (9)	4.18 (11)	6.22 (18)	2.08 (21)	0.86 (5)	2.52 (1)	99.34	2.21 (6)	1.162

* Three duplicate experiments with similar bulk concentrations of volatile components; n - number of electron microprobe analyses; [a] initial concentration of Cl in HCl solution charged into the capsules; [b] the amount of added CO_2 corrected by adding 0.25 ± 0.10 mg (Botcharnikov *et al.*, 2006); [c] AgCl, AgCl+H_2O+CO_2 and AgCl+CO_2 were added as fluid sources with bulk Cl content about 10, 8 and 10 wt.% in runs Cl245, ClC174 and ClC175, respectively; [d] water content of the glasses is determined by KFT method and corrected for unextracted water by adding 0.13 wt.% according to Behrens & Stuke (2003).

Table 3. The composition of the fluid phase and CO_2 content of the glasses (1σ error).

Sample	Glass ini, mg [a] (±0.02)	CO_2 fin, mg[b] (±0.02)	H_2O-Cl fin, mg [c] (±0.02)	CO_2^{mol} melt, ppm	CO_2^{carb} melt, ppm	CO_2^{tot} melt, ppm	XH_2O^{fl}	XCO_2^{fl}	XCl^{fl}
Cl130	50.40	–	–	–	–	–	0.997 (52)	–	0.003 (7)
Cl131	50.22	–	–	–	–	–	0.983 (57)	–	0.017 (8)
Cl239	50.10	–	–	–	–	–	0.942 (53)	–	0.058 (9)
Cl240	50.29	–	–	–	–	–	0.895 (71)	–	0.105 (10)
Cl243	49.85	–	–	–	–	–	0.808 (75)	–	0.192 (19)
Cl245	49.73	–	–	–	–	–	0.200 (200)	–	0.800 (200)
Cl84	49.83	–	–	–	–	–	0.996 (48)	–	0.004 (7)
Cl85	49.60	–	–	–	–	–	0.991 (53)	–	0.009 (8)
Cl86	49.20	–	–	–	–	–	0.976 (60)	–	0.024 (9)
ClC148	50.38	0.78	0.45	23 (13)	384 (80)	407 (81)	0.836 (44)	0.143 (6)	0.021 (6)
ClC149	50.02	0.86	0.68	21 (10)	339 (90)	360 (91)	0.843 (32)	0.141 (5)	0.016 (5)
ClC150	49.90	0.82	0.55	16 (9)	301 (86)	317 (86)	0.841 (29)	0.144 (5)	0.015 (5)
ClC151	49.13	0.99	0.92	18 (9)	343 (92)	361 (92)	0.845 (29)	0.154 (5)	0.001 (4)
ClC152	50.08	0.88	0.75	21 (10)	359 (116)	380 (116)	0.863 (32)	0.134 (4)	0.003 (4)
ClC153	50.26	0.88	0.45	20 (13)	439 (118)	459 (119)	0.857 (28)	0.137 (4)	0.006 (4)
ClC154	49.97	0.95	0.65	18 (14)	777 (120)	795 (121)	0.633 (32)	0.239 (9)	0.128 (15)
ClC171	50.59	0.93	0.19	–	521 (89)	521 (89)	0.763 (37)	0.198 (7)	0.039 (6)
ClC172	50.56	1.06	0.10	–	569 (121)	569 (121)	0.785 (34)	0.192 (6)	0.024 (5)
ClC173	50.08	0.86	0.20	8 (8)	499 (125)	507 (125)	0.731 (43)	0.196 (8)	0.074 (10)
ClC174	50.14	1.29	0.00	11 (8)	188 (68)	199 (68)	0.400 (200)	0.100 (100)	0.500 (200)
ClC175	50.44	2.26	0.00	24 (8)	60 (67)	84 (67)	0.150 (150)	0.050 (50)	0.800 (200)

[a] Initial mass of the glass needed for mass balance calculations; [b] the amount of CO_2 measured after piercing of the capsules freezed by liquid nitrogen; [c] the amount of the fluid (H_2O and/or Cl-bearing compounds) after heating of the pierced capsules at 110 °C for 3 min.

quenched products were composed of bubble- and crystal-free glasses + non-quenchable fluid phase(s). However, in the experimental runs with ClC171-ClC175 samples, all experimental glasses contained small but numerous bubbles and sometimes quench crystals, indicating that the rapid quench was not completely successful. Thus, the analytical results on volatile concentrations in those samples may be affected by the presence of quench phases (see discussion below). The quench crystals were too small to be analyzed with electron microprobe but based on the back-scattered electron images they may be composed of magnetites and clinopyroxenes.

3.1. Electron microprobe

A Cameca SX-100 electron microprobe was used to analyze the compositions of all experimental glasses. Only crystal- and bubble-free areas of the samples with quench phases were analyzed with electron microprobe. Glass analyses were conducted with 15 kV acceleration potential, 4 nA beam current, a defocused electron beam (10–20 μm diameter) and peak counting times of 8 s for major elements. Sodium and potassium were analyzed first for 4 s to minimize their migration. The used beam current and size provided analytical conditions with a curent density significantly below 0.5 nA/μm^2, according to the data of (Morgan & London, 2005). Such low current densities are required for accurate and reliable analyses of hydrous silicate glasses, minimizing the loss of alkalis (Morgan & London, 2005). No significant alkali loss was determined with the chosen analytical conditions (*i.e.*, the change in Na and K concentrations with time is within the analytical uncertainty of 0.5 wt.% for Na and 0.2 wt.% for K). Chlorine was measured as the last element with an electron beam of 30 nA and with a counting time of 60 s. NaCl was used as a standard for Cl analysis. Multiple measurements were made for each sample (8–30 analyses, Table 2) to check for reproducibility of the analyses and homogeneity of Cl distribution in the experimental glasses. The detection limit for Cl was about 300 ppm by weight. The microprobe analyses were not calibrated against additional standard silicate glasses with known amount of chlorine. However, standards with low levels of the required trace element are not recommended because of possible serious uncertainties in the concentration and homogeneity of trace components (Robinson *et al*., 1998). The analytical conditions were identical for all measured glasses, and the compositions of major elements were similar for most samples except samples Cl245, ClC174, and ClC175, having lower concentrations of Fe, Ca, Na and K due to loss into the fluid phase(s) during the experiment. It implies that, even

if the absolute values of Cl concentration may have a systematic error due to matrix effects, the relative changes are measured accurately.

3.2. Determination of H_2O and CO_2 contents of the glasses

The bulk water content of the quenched glasses was determined by KFT (Table 2). All water analyses were corrected by adding 0.13 wt.% H_2O according to Behrens & Stuke (2003) who noted that there is a systematic error in unextracted water in KFT analyses. As mentioned above, ClC171-ClC175 samples contained small numerous bubbles that could influence the determined concentrations of H_2O in the glasses. However, the other samples were almost bubble-free, indicating that the bubbles in ClC171-ClC175 samples were produced during quench. Hence, the bulk composition of the system "silicate glass + dissolved volatile" should not be significantly changed by the formation of quench bubbles. The amount of quench crystals is very small (< 1 vol.%). Due to the fact that the KFT analysis provides data on the bulk composition of the sample, we believe that the KFT analyses for ClC171-ClC175 samples were not dramatically affected by the presence or absence of quench phases.

The CO_2 content of the glasses was measured by FTIR spectroscopy as described in detail by (Botcharnikov *et al*., 2006). Doubly polished glass plates of ~ 80–140 μm thickness were measured with a Bruker IFS88 FTIR spectrometer coupled with IR-Scope II microscope (operation conditions: MCT narrow range detector; globar light source and KBr beamsplitter; spectral resolution 2 cm^{-1}). Densities of hydrous andesitic glasses were estimated from the equation proposed by (Ohlhorst *et al.*, 2001) for the same andesitic composition ($\rho = [-18.4 \pm 2.0] \cdot C_{H2O}{}^{tot} + [2661 \pm 7]$, where ρ is a density in g/L, C_{H2O}^{tot} is the total water content of the glass in wt.%). Typically 50 scans were used for analyses of each glass with a spot size of approximately 100×100 μm. However, glasses with quenched phases were analyzed with a spot size of 50×50 μm. To minimize the contribution of atmospheric CO_2 to the MIR spectra, the sample stage of the IR microscope was shielded and purged with dry air (see Botcharnikov *et al*., 2006) for a discussion of the precision and accuracy of the measurements). The concentrations of carbon species were determined from the heights of baseline-corrected peaks of molecular CO_2 (CO_2^{mol}) at 2350 cm^{-1} and of carbonate CO_2 (CO_2^{carb}) at 1430 cm^{-1}. Due to relatively low bulk CO_2 concentrations (about 80–800 ppm) and high H_2O content (2–6 wt.%), the intensity of the H_2O band at 1630 cm^{-1} was very high, completely overlapping the carbonate band at 1530 cm^{-1} and significantly influencing the band at 1430 cm^{-1}. The base-line correction of the spectra was performed by the subtraction of a spectrum of volatile-free andesitic glass, synthesized at 1600 °C and atmospheric pressure, from the sample spectra. Next, tangential baselines were fitted to both band systems as described by (Botcharnikov *et al*., 2006). Due to very low contents of carbon in the glasses and the effect of H_2O band on the CO_2^{carb} peak (see also King *et al*., 2002, 2004) even after subtraction of a reference spectrum, the IR spectroscopic measurements have a large uncertainty in carbon species concentrations. To quantify the concentrations of CO_2^{mol} and CO_2^{carb} in the glasses, we used the absorption coefficient ε_{2350} of 1214 ± 78 $L \cdot cm^{-1} \cdot mol^{-1}$ (Behrens et al., 2004b) for CO_2^{mol} and the absorption coefficient ε_{1430} of 170 $L \cdot cm^{-1} \cdot mol^{-1}$ for CO_2^{carb} (Behrens *et al*., 2004a). The possible errors associated with those coefficients applied to the andesitic composition are also discussed by (Botcharnikov *et al*., 2006).

We tried to avoid quench phases being included in the analyses but it was not always possible. The effect of small amount of tiny quench crystals should not be significant in IR measurements but the presence of gaseous phase in the bubbles can be dramatic for the carbon species determination. Thus, we do not discuss the speciation of carbon in the experimental glasses in this paper. It must be noted, however, that the effect of quench bubbles should be mostly related to the molecular CO_2. The measured concentrations of CO_2^{mol} in most samples were significantly lower (approximately 10 relative % in total) than the concentrations of CO_2^{carb} (see Table 3) indicating that the determined total CO_2 contents of the glasses were not significantly influenced by the incorporation of quench phases in the IR analysis (the concentrations of CO_2^{mol} are within the errror of the bulk CO_2). Furthermore, it has to be emphasized that contributions of gaseous CO_2 to the CO_2^{mol} band would result in splitting of the peak due to rotation-vibration coupling. Such splitting was not observed in our spectra.

3.3. Determination of fluid composition

The composition of the fluid phase was determined by two methods: (1) the mass proportion of gaseous CO_2 was measured by a conventional weight-loss method (freezing-piercing-heating; see *e.g.*, Botcharnikov *et al*. (2006) for detail); (2) the composition of the H_2O- and Cl-bearing fluid was constrained from mass balance, knowing the initial amounts of fluid components and the final concentrations of H_2O and Cl in the glasses. The mass-balance calculations were necessary for determining the fluid composition, because with the experimental strategy used in this study, the exact composition of the fluid phase could not be measured directly (small amounts of fluid were used to minimize the effect of incongruent dissolution of the silicate components in the fluid) and because the fluid phase could not be quenched after the experiment. The quenched fluids produced condensed and non-condensed phases on quench. We assumed that the amount of gas released on capsule piercing after freezing with liquid nitrogen and warming up to room temperature is composed mostly of CO_2 as non-condensable fluid component in all CO_2-bearing experiments except ClC174 and ClC175. These two samples contained large amounts of AgCl as a fluid source, probably resulting in the formation of Cl-rich brine and excess Cl-rich non-condensable gas phase (see also Table 3 and discussion below). It is evident from the amount of fluid released on piercing (Table 3), significantly exceeding the expected amount of gaseous CO_2.

The amounts of fluid released on capsule heating at 110 °C represent probably only part of the H_2O- and Cl-bearing fluid phase(s) which can be evaporated by heating. The rests of the fluid (for instance, Cl-rich brine) remained inside the capsules limiting the significance of the obtained data on fluid composition.

For the mass balance we used the initial amounts of the silicate glass, the amounts and concentration of Cl and H_2O in HCl and AgCl sources, the concentration of dissolved H_2O and Cl in the glass and the final amount of CO_2 in the fluid phase after the experiment. The concentration of CO_2 dissolved in the glass was less than 800 ppm and we have neglected it in mass-balance calculations. It is emphasized that only the bulk mass amounts of H_2O and Cl in the fluid phase(s) could be calculated, regardless of the presence of one or two immiscible fluids during the run.

The compilation of both methods provided data on the bulk mole fractions of H_2O, Cl and CO_2 in the fluid phase (hereafter presented as mole fractions Xi^{fl}) in equilibrium with the andesitic melt, assuming for simplicity that Cl bonds to monovalent cations only.

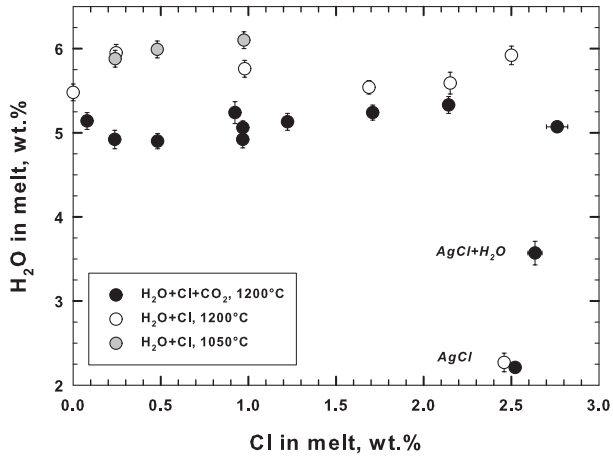

Fig. 1. The concentrations of H_2O and Cl dissolved in andesitic melt at 200 MPa. Note significant difference between CO_2-free (white and grey circles) and CO_2-bearing (black circles) systems. The value of pure H_2O solubility in andesitic melt at 200 MPa is after Botcharnikov *et al.* (2006).

4. Results

The results of the solubility experiments are summarized in Tables 2 and 3. The composition of most experimental melts was homogeneous and similar to the starting glass composition (Tables 1 and 2). The molar Al_2O_3 / ($CaO+Na_2O+K_2O$) ratios (A/CNK) are about 0.820–0.850, a value which is close to the value of 0.850 of the starting glass. The compositional variations of all elements in the glasses on an anhydrous basis are within the analytical uncertainty (Table 2). The exceptions are Cl245, ClC174 and ClC175 samples with A/CNK values of 1.166, 1.009, and 1.162, respectively. The decrease in FeO^{tot} concentration in those samples correlates with the decrease in CaO, Na_2O and K_2O concentrations. This indicates that the low FeO^{tot} concentration in the glasses was not due to Fe loss into the capsules but was related to a partitioning of Fe, Ca, Na and K from the silicate melt into the Cl-rich fluid phase.

4.1. Concentrations of H_2O, Cl and CO_2 dissolved in the melt

The relationship between dissolved concentrations of H_2O (H_2O^{melt}) and Cl (Cl^{melt}) in the melt at 200 MPa is illustrated in Fig. 1. The CO_2-free system at 1200 °C and 1050 °C shows H_2O solubility values of about 5.5–6.0 wt.% with increasing Cl concentration up to about 2.5 wt.% Cl. The nominally dry experiment Cl245, with only AgCl as a fluid source, shows low H_2O content in the melt of about 2.1 wt.% with Cl content of 2.5 wt.%. This amount of water is believed to be mostly generated during the experiment due to the reaction between oxygen present in the system and hydrogen diffusing from the vessel into the capsule (*e.g.*, reduction of Fe_2O_3 to FeO in the melt). The initial amount of water incorporated in AgCl and adsorbed on the glass powder is significantly lower than that measured in the melt.

Addition of CO_2 to the system has a significant effect on the concentrations of dissolved H_2O as shown in Fig. 1. At a given initial bulk HCl concentration in the system, the H_2O content of the melt is systematically lower by approximately 1 wt.% H_2O with a dilution of the fluid by the CO_2. This difference is smaller in two CO_2-free and two CO_2-bearing samples containing about 1.7 and 2.1 wt.% Cl in the melt. Another important observation is that the concentrations of Cl in the melts are not considerably affected by added CO_2: at a given HCl content in the system the Cl^{melt} remains almost constant although H_2O^{melt} decreases (Fig. 1). The ClC174 and ClC175 samples show low H_2O solubility values of 3.6 and 2.2 wt.%, respectively, at almost constant Cl^{melt} of about 2.5–2.6 wt.%. Both samples have higher final amounts of H_2O compared with the initially charged H_2O (2 and ~ 0 wt.% bulk initial H_2O, respectively). Remarkable is that the amounts of H_2O and Cl dissolved in the melt coexisting with Cl-rich CO_2-free (Cl245) and CO_2-bearing (ClC175) fluids are identical within the error. It implies that CO_2 has little effect on the concentrations of H_2O and Cl in the melt which coexists with extremely Cl-rich fluid(s).

The concentrations of dissolved CO_2 are listed in Table 3 and shown in Fig. 2 and 3 as a function of H_2O and Cl contents in the melt, respectively. The relationship between H_2O^{melt} and CO_2 in the melt (CO_2^{tot}) is in a good agreement with our previous data for the Cl-free system (Botcharnikov *et al.*, 2006) as illustrated in Fig. 2. All samples with Cl content of the melt below ~ 2.3 wt.% follow, in general, the H_2O-CO_2 solubility trend at 200 MPa and 1200 °C. However, the Cl-rich ClC174 and ClC175 samples depart from the observed trend. Both samples have high amounts of AgCl as a fluid source, resulting in the formation of Cl-rich fluid phase(s). We suggest that the decomposition of AgCl produces brine and Cl-bearing

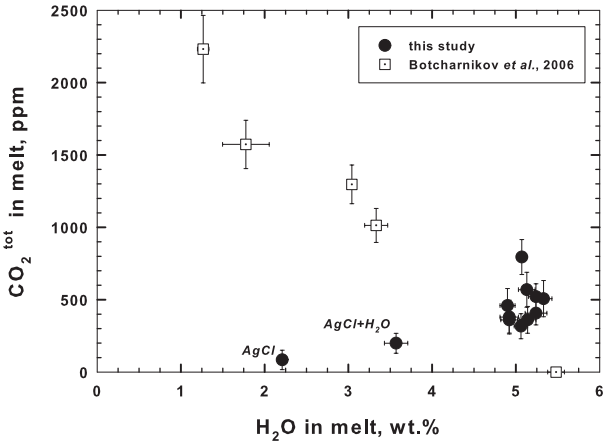

Fig. 2. The relationship between H_2O and CO_2 concentrations of the melt. Dotted squares are the data for Cl-free andesitic magma at 1200 °C and 200 MPa after Botcharnikov *et al.* (2006).

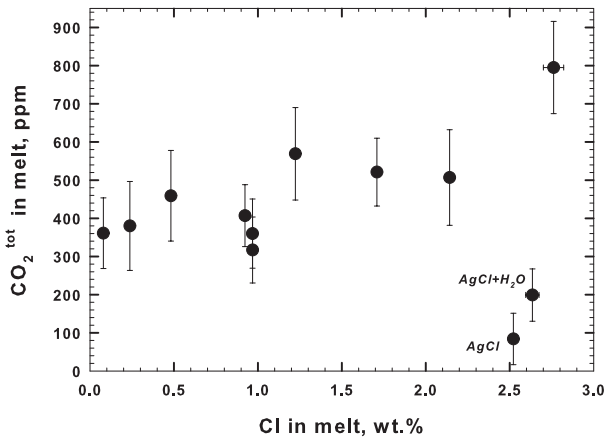

Fig. 3. The CO_2 content of the melt as a function of Cl concentration in the melt.

gaseous phase (probably Cl_2 and/or HCl) as mentioned above. As a consequence, the amounts of other volatile components in the fluid(s), *i.e.*, H_2O and CO_2, are significantly diluted, resulting in lower solubility in coexisiting silicate melt. The CO_2^{tot} versus Cl^{melt} relationship, plotted in Fig. 3, shows no obvious correlation between these two volatile components. The concentration of CO_2 in the glass remains similar within the analytical uncertainty for most samples with increasing Cl content. However, three samples, *i.e.*, ClC154, ClC174, and ClC175 (samples with Cl^{melt} > 2.5 wt.%), show significant deviation in the amounts of dissolved CO_2.

4.2. Relationship between fluid composition and solubility of H_2O-, Cl- and CO_2-bearing fluids in andesitic melt

The mole fractions of H_2O, Cl and CO_2, calculated by mass balance, are listed in Table 3 and plotted in Fig. 4–6. The errors in mass-balance calculations are related to the uncertainties of the weight-loss method and the analytical

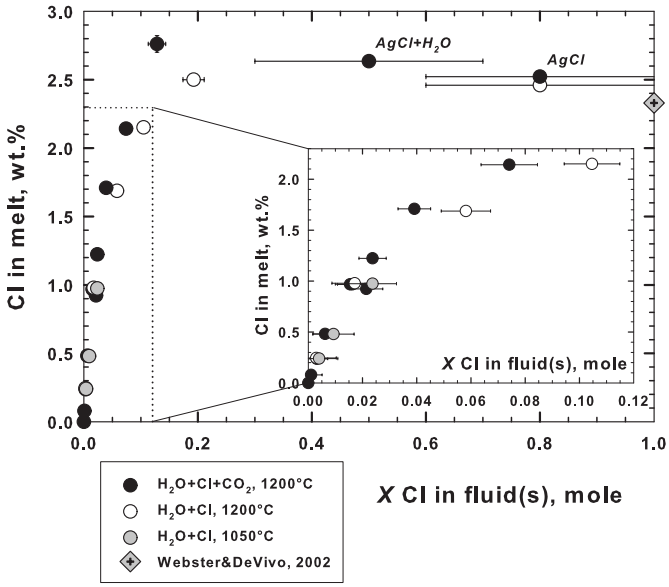

Fig. 4. The concentrations of Cl in the melt as a function of bulk Cl content in the fluid phase(s). The inlet shows the enlarged part of the diagram outlined by the dotted lines.

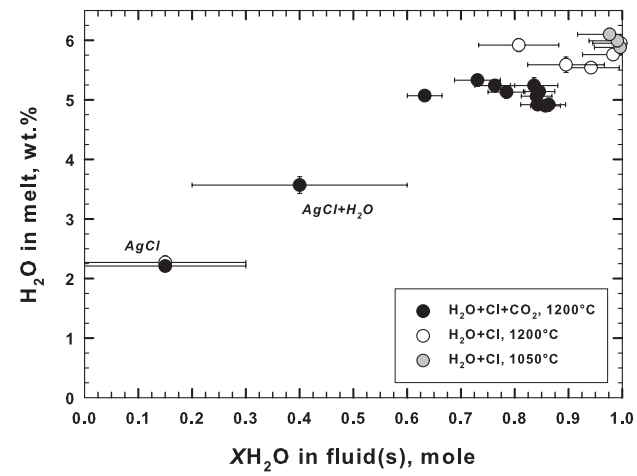

Fig. 5. The concentration of H_2O in the melt versus mole fraction of H_2O in the fluid(s).

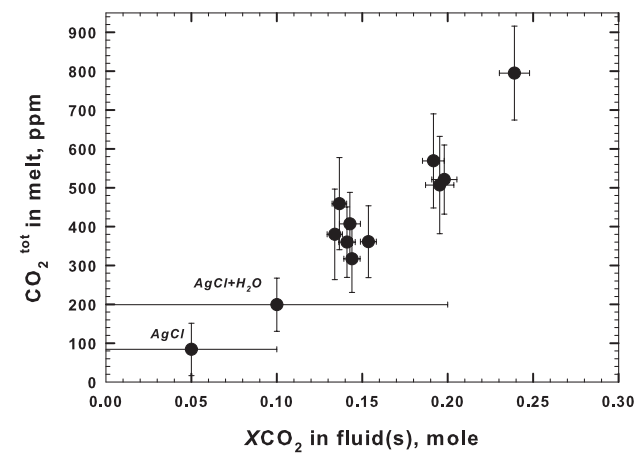

Fig. 6. Relationship between CO_2 content of the melt and XCO_2^{fl}.

techniques. The composition of the fluid in Cl245, ClC174 and ClC175 samples could not be reliably constrained from mass-balance calculations due to unknown amounts of generated water and Cl-rich gaseous phase during the experiment. We suggest that the melt-fluid system with high Cl content was composed of the andesitic melt and Cl-rich brine (± Cl_2 ± HCl ± CO_2 gaseous phase) at the investigated conditions, according to the data and models of Webster *et al*. (1999) and Webster & De Vivo (2002) for mafic melts. Thus, for simplicity, we assumed that the $X\mathrm{Cl}^{\mathrm{fl}}$ for the samples Cl245 and ClC175 is close to ~ 0.8, while $X\mathrm{H_2O}^{\mathrm{fl}}$ and $X\mathrm{CO_2^{fl}}$ are about 0.2 and 0 for Cl245 and 0.15 and 0.05 for ClC175, respectively. The experimental data on immiscibility in H_2O-Cl-bearing fluid systems show that the partitionig of water into the brine can be significant. According to the the data for the H_2O-(Na,K)Cl fluids reported by Chou, (1987) and Anderko & Pitzer (1993a,b), the mole fraction of water in the brine at 200 MPa and 1200 °C is estimated to be up to ~ 40–50 mole%. Hence, we assumed that the ClC174 sample might contain approximately $X\mathrm{Cl}^{\mathrm{fl}} = 0.5$, $X\mathrm{H_2O}^{\mathrm{fl}} = 0.4$ and $X\mathrm{CO_2}^{fl} = 0.1$ in the fluid.

The relationship between Cl content in the melt and the mole proportion of Cl in the fluid phase is shown in Fig. 4. Chlorine concentration in the melt increases non-linearly with Cl in the CO_2-free fluid, reaching an almost constant value of 2.5 wt.% with $X\mathrm{Cl}^{\mathrm{fl}} > 0.2$. The maximum solubility of Cl in our andesitic melt is predicted to be about 2.43 wt.% according to the model of Webster & De Vivo (2002) which is in a good agreement with the highest value measured in our samples (see Fig. 4). In general, in the CO_2-bearing systems, the $\mathrm{Cl}^{\mathrm{melt}}$ increases with $X\mathrm{Cl}^{\mathrm{fl}}$ similar to the CO_2-free systems. However, at a given $X\mathrm{Cl}^{\mathrm{fl}}$, the $\mathrm{Cl}^{\mathrm{melt}}$ is higher at $X\mathrm{Cl}^{\mathrm{fl}} > 0.03$ and even shows a maximum at $X\mathrm{Cl}^{\mathrm{fl}} \sim 0.2$ (up to ~ 2.8 wt.% Cl) in CO_2-bearing melts.

The relationships between $X\mathrm{H_2O}^{\mathrm{fl}}$ and $\mathrm{H_2O}^{\mathrm{melt}}$ and $X\mathrm{CO_2^{fl}}$ and $\mathrm{CO_2^{melt}}$ are illustrated in Fig. 5 and 6, respectively, indicating positive dependences for both H_2O and CO_2.

5. Discussion

The data on H_2O and CO_2 partitioning between fluid and melt obtained in this study are in a good agreement with our previous data for the same andesitic system (Cl-free system) with higher amounts of CO_2 (Botcharnikov *et al*., 2006). The general $\mathrm{H_2O}^{\mathrm{melt}}$ *vs.* $\mathrm{CO_2^{melt}}$ trend (Fig. 2) indicates that the observed decrease in concentrations of H_2O dissolved in the melt is attributed to the decrease in water fugacity in the fluid phase with increasing $X\mathrm{CO_2^{fl}}$. This relationship agrees also with the literature data for other silicate melt compositions (*e.g.*, Blank *et al.*, 1993; Dixon *et al.*, 1995; Tamic *et al.*, 2001; Behrens *et al.*, 2004a; Botcharnikov *et al.*, 2005a). The presence of small amounts of Cl in the system has no detectable effect on the $\mathrm{H_2O}^{\mathrm{melt}}$ *vs.* $\mathrm{CO_2^{melt}}$ trend, at least at the studied bulk H_2O and CO_2 contents and at a pressure of 200 MPa. The reason for significant differences from the trend for ClC174 and ClC175 samples becomes clear if $X\mathrm{H_2O}^{\mathrm{fl}}$ and $X\mathrm{CO_2^{fl}}$ prevailing in these experiments are taken into account, as shown in Fig. 5 and 6. It is evident that the low concentrations of dissolved H_2O and CO_2 are directly related to the low mole fractions of these volatiles in the fluid phase(s). The dependence presented in Fig. 6 also implies that CO_2 behaves almost idealy in the melt-fluid(s) system, *i.e.*, CO_2 concentration in the melt increases almost linearly with CO_2 concentration in the fluid.

On the other hand, the evolution of $\mathrm{H_2O}^{\mathrm{melt}}$ as a function of $X\mathrm{H_2O}^{\mathrm{fl}}$ differs if H_2O is diluted by adding Cl or CO_2. In the case of added CO_2, water partitioning between melt and fluid also shows a nearly ideal behavior in andesitic melts at 200 MPa (e.g, (Botcharnikov *et al.*, 2006), similar to that of CO_2. In the case of added HCl, the H_2O dissolved in the melt does not change significantly with decreasing $X\mathrm{H_2O}^{\mathrm{fl}}$ for small-to-intermediate amounts of Cl and a dramatic decrease of $\mathrm{H_2O}^{\mathrm{melt}}$ with decreasing $X\mathrm{H_2O}^{\mathrm{fl}}$ is observed at high added Cl contents (Fig. 5). This is consistent with the relationships between the concentrations of H_2O and Cl in the melt shown in Fig. 1 (see also Fig. 4), indicating a strong non-ideality of the H_2O-salt-bearing fluid phase, resulting in the formation of two immiscible fluids, *i.e.*, low-salinity vapor and brine, at high bulk Cl contents (*e.g.*, Carroll & Webster, 1994; Webster & De Vivo, 2002). The complex non-linear relationships between $\mathrm{H_2O}^{\mathrm{melt}}$ and $\mathrm{Cl}^{\mathrm{melt}}$ as well as between X_{Cl}^{fl} and $\mathrm{Cl}^{\mathrm{melt}}$ imply that the activity coefficients of both H_2O and Cl in the Cl-rich system may increase significantly, positively affecting the solubility of H_2O and Cl in the melt with increasing $X\mathrm{Cl}^{\mathrm{fl}}$. This effect is probably most pronounced at the conditions which are very close to the P-T-X immiscibility region (where X is a salt concentration in the fluid; for more detail see also models of Shinohara *et al.* (1989) and Webster & De Vivo (2002).

The added amounts of CO_2 have almost no effect on the dissolved concentrations of Cl in the melt. Moreover, CO_2 does not significantly influence the $X\mathrm{Cl}^{\mathrm{fl}}$ *versus* $\mathrm{Cl}^{\mathrm{melt}}$ relationship at least up to $X\mathrm{Cl}^{\mathrm{fl}} < 0.03$ as illustrated in Fig. 4. However, at higher bulk Cl in the system, the effect of CO_2 becomes detectable, resulting in higher $\mathrm{Cl}^{\mathrm{melt}}$ concentrations at a given $X\mathrm{Cl}^{\mathrm{fl}}$ (compare Cl243 sample with $\mathrm{Cl}^{\mathrm{melt}}$ = 2.5 wt.% and ClC154 sample with $\mathrm{Cl}^{\mathrm{melt}}$ = 2.8 wt.% in Fig. 4 and in Table 2). The observed effect is the opposite of that which can be expected from the simple dilution of the H_2O-Cl-bearing fluid by the CO_2 (a decrease in $\mathrm{Cl}^{\mathrm{melt}}$ would be expected). On the other hand, it is known that CO_2 may affect significantly the mixing properties of H_2O-salt-bearing fluids. The effect is related to an enlargement of the P-T-X range of the immiscibility gap in H_2O-salt-bearing fluid systems with addition of CO_2 (for more detail see experimental results and models of *e.g.*, Joyce & Holloway, 1993; Duan *et al.*, 1995; Shmulovich & Graham, 1999; 2004). This also indicates that the activity coefficient of Cl in the fluid phase(s) could increase, resulting in higher concentrations of $\mathrm{Cl}^{\mathrm{melt}}$ at a given $X\mathrm{Cl}^{\mathrm{fl}}$. A positive effect of CO_2 on the concentration of Cl dissolved in rhyolitic melt was previously reported by Webster & Holloway (1988). The authors explained the effect by a decrease in the mean dielectric constant of the fluid phase and an increase in the activity of Cl in the fluid.

Based on the obtained results we can conclude that CO_2 partitioning between the coexisting melt and fluid phase(s) is controlled by the fugacity of CO_2 in the fluid(s) and by the CO_2 capacity of the melt. The non-ideal behavior of the H_2O-salt-bearing system is expected at our experimental conditions, which is confirmed by the experiments. However, we have observed an additional significant influence of CO_2 on the mixing properties of the H_2O-Cl-bearing fluids which were in equilibrium with the andesitic melt. The interesting and important consequence of those results for the interpretation of natural systems is that H_2O^{melt} may remain nearly constant with decreasing XH_2O^{fl} in Cl-rich magmas. It implies that the measured concentrations of H_2O and CO_2 in melt inclusions may not always be used as quantitative indicators of magma storage conditions if the concentrations of other volatiles are not taken into account. In other words, Cl-rich non-ideal systems may provide higher estimates for the magmatic pressures at the time of melt inclusion entrapment if the calculations are based on pure H_2O-CO_2-silicate melt system (see *e.g.*, Papale *et al*., 2006). The effect is expected to be most pronounced at low pressures and H_2O contents and/or high Cl and CO_2 concentrations in magmatic system. Additional influences on the mixing properties of the fluids are expected from the salt composition of the fluid phase, *i.e.*, from relative abundances of mono- and divalent cations (for instance, H_2O-CO_2-$CaCl_2$-bearing fluids are characterized by larger immiscibility gap than H_2O-CO_2-NaCl-bearing fluids at given T and P (Shmulovich & Graham, 2004). Thus, the effect of CO_2 on the solubility behavior of H_2O-salt-bearing fluids should be more efficient in the systems with fluids coexisting with mafic rather than with felsic melts.

Acknowledgements: S. Kohn, J. Blundy and M. Walter are acknowledged for the organization of this special issue of EJM. We thank S. Feig and O. Beermann for the help with the realization of the experiments. O. Diedrich is acknowledged for the preparation of samples for analyses. P. King and J. Webster provided constructive and helpful comments on the experimental results and interpretation of the data that improved the quality of the paper. This work was funded by the DFG (project Ho1337/11).

References

Anderko, A. & Pitzer, K.S. (1993a): Phase-equilibria and volumetric properties of the systems KCl-H_2O and NaCl-KCl-H_2O above 573 K - Equation of state representation. *Geochim. Cosmochim. Acta*, **57**, 4885-4897.

—, — (1993b): Equation-of-state representation of phase-equilibria and volumetric properties of the system NaCl-H_2O above 573 K. *Geochim. Cosmochim. Acta*, **57**, 1657-1680.

Baker, D.R., Freda, C., Brooker, R.A., Scarlato, P. (2005): Volatile diffusion in silicate melts and its effects on melt inclusions. *Ann. Geophys.*, **48**, 699-717.

Behrens, H. & Stuke, A. (2003): Quantification of H_2O contents in silicate glasses using IR spectroscopy - a calibration based on hydrous glasses analyzed by Karl-Fischer titration. *Glass Sci. Technol.*, **76**, 176-189.

Behrens, H., Ohlhorst, S., Holtz, F., Champenois, M. (2004a): CO_2 solubility in dacitic melts equilibrated with H_2O-CO_2 fluids: Implications for modeling the solubility of CO_2 in silicic melts. *Geochim. Cosmochim. Acta*, **68**, 4687-4703.

Behrens, H., Tamic, N., Holtz, F. (2004b): Determination of the molar absorption coefficient for the infrared absorption band of CO_2 in rhyolitic glasses. *Am. Mineral.*, **89**, 301-306.

Behrens, H., Zhang, Y., Xu, Z. (2004c): H_2O diffusion in dacitic and andesitic melts. *Geochim. Cosmochim. Acta*, **68**, 5139-5150.

Berndt, J., Liebske, C., Holtz, F., Freise, M., Nowak, M., Ziegenbein, D., Hurkuck, W., Koepke, J. (2002): A combined rapid-quench and H_2-membrane setup for internally heated pressure vessels: Description and application for water solubility in basaltic melts. *Am. Mineral.*, **87**, 1717-1726.

Blank, J.G., Stolper, E.M., Carroll, M.R. (1993): Solubilities of carbon-dioxide and water in rhyolitic melt at 850 °C and 750 bars. *Earth Planet. Sci. Lett.*, **119**, 27-36.

Boettcher, S.L., Guo, Q., Montana, A. (1989): A simple device for loading gases in high-pressure experiments. *Am. Mineral.*, **74**, 1383-1384.

Botcharnikov, R.E., Behrens, H., Holtz, F., Koepke, J., Sato, H. (2004): Sulfur and chlorine solubility in Mt. Unzen rhyodacitic melt at 850 °C and 200 MPa. *Chem. Geol.*, **213**, 207-225.

Botcharnikov, R., Freise, M., Holtz, F., Behrens, H. (2005a): Solubility of C-O-H mixtures in natural melts: new experimental data and application range of recent models. *Ann. Geophys.*, **48**, 633-646.

Botcharnikov, R.E., Koepke, J., Holtz, F., McCammon, C., Wilke, M. (2005b): The effect of water activity on the oxidation and structural state of Fe in a ferro-basaltic melt. *Geochim. Cosmochim. Acta*, **69**, 5071-5085.

Botcharnikov, R.E., Behrens, H., Holtz, F. (2006): Solubility and speciation of C-O-H fluids in andesitic melt at T = 1100−1300 °C and P = 200 and 500 MPa. *Chem. Geol.*, **229**, 125-143.

Botcharnikov, R.E., Holtz, F., Almeev, R.R., Sato, H., Behrens, H. (in press): Storage conditions and evolution of andesitic magma prior to the 1991-95 eruption of Unzen volcano: Constraints from natural samples and phase equilibria experiments. *J. Volcanol. Geotherm. Res.*

Carroll, M.R. & Webster, J.D. (1994): Solubilities of sulfur, noble gases, nitrogen, chlorine, and fluorine in magmas, *in* "Volatiles in magmas", R. Carroll Michael, R. Holloway John, eds. Mineralogical Society of America, Washington, DC, United States, **30**, 231-279.

Chou, I.M. (1987): Phase-relations in the system NaCl-KCl-H_2O. III: Solubilities of halite in vapor-saturated liquids above 445 °C and redetermination of phase-equilibrium properties in the system NaCl-H_2O to 1000 °C and 1500 bars. *Geochim. Cosmochim. Acta*, **51**, 1965-1975.

Dixon, J.E., Stolper, E.M., Holloway, J.R. (1995): An experimental study of water and carbon dioxide solubilities in mid ocean ridge basaltic liquids. I: Calibration and solubility models. *J. Petrol*, **36**, 1607-1631.

Duan, Z.H., Moller, N., Weare, J.H. (1995): Equation of state for the NaCl-H_2O-CO_2 system - prediction of phase-equilibria and volumetric properties. *Geochim. Cosmochim. Acta*, **59**, 2869-2882.

Gill, J.B. (1981): Orogenic andesite and plate tectonics. Springer, p. 385.

Holtz, F., Sato, H., Lewis, J., Behrens, H., Nakada, S. (2005): Experimental petrology of the 1991-1995 Unzen dacite, Japan. Part I: Phase relations, phase composition and pre-eruptive conditions. *J. Petrol.*, **46**, 319-337.

Joyce, D.B. & Holloway, J.R. (1993): An experimental determination of the thermodynamic properties of H_2O-CO_2-NaCl fluids at high-pressures and temperatures. *Geochim. Cosmochim. Acta*, **57**, 733-746.

King, P.L., Vennemann, T.W., Holloway, J.R., Hervig, R.L., Lowenstern, J.B., Forneris, J.F. (2002): Analytical techniques for volatiles: A case study using intermediate (andesitic) glasses. *Am. Miner*. **87**, 1077-1089.

King, P.L., McMillan P. F., Moore, G. (2004): Infrared spectroscopy of silicate glasses with application to natural systems, *in* "Infrared spectroscopy in geochemistry, exploration geochemistry and remote sensing", P.L. King, M.S.Ramsey, G.A. Swayze, eds. Mineralogical Association of Canada, Short course, **33**, 93-133.

Liu, Y., Zhang, Y., Behrens, H. (2005): Solubility of H_2O in rhyolitic melts at low pressures and a new empirical model for mixed H_2O-CO_2 solubility in rhyolitic melts. *J. Volcanol. Geotherm. Res.*, **143**, 219-235.

Mathez, E.A. & Webster, J.D. (2005): Partitioning behavior of chlorine and fluorine in the system apatite-silicate melt-fluid. *Geochim. Cosmochim. Acta*, **69**, 1275-1286.

Moretti, R. & Papale, P. (2004): On the oxidation state and volatile behavior in multicomponent gas-melt equilibria. *Chem. Geol.*, **213**, 265-280.

Moretti, R., Papale, P., Ottonello, G. (2003): A model for the saturation of C-O-H-S fluids in silicate melts, *in* "Volcanic degassing", C. Oppenheimer, P.D.M., J. Barclay eds. Geol. Soc. Spec. Publ., London, 213, 81-101.

Morgan, G.B. & London, D. (2005): Effect of current density on the electron microprobe analysis of alkali aluminosilicate glasses. *Am. Mineral.*, **90**, 1131-1138.

Nakada, S. & Motomura, Y. (1999): Petrology of the 1991-1995 eruption at Unzen: effusion pulsation and groundmass crystallization. *J. Volcanol. Geotherm. Res.*, **89**, 173-196.

Newman, S. & Lowenstern, J.B. (2002): VOLATILECALC: a silicate melt-H_2O-CO_2 solution model written in Visual Basic for excel. *Comput. Geosci.*, **28**, 597-604.

Nowak, M., Schreen, D., Spickenbom, K. (2004): Argon and CO_2 on the race track in silicate melts: A tool for the development of a CO_2 speciation and diffusion model. *Geochim. Cosmochim. Acta*, **68**, 5127-5138.

Ohlhorst, S., Behrens, H., Holtz, F. (2001): Compositional dependence of molar absorptivities of near-infrared OH- and H_2O bands in rhyolitic to basaltic glasses. *Chem. Geol.*, **174**, 5-20.

Papale, P. (1999): Modeling of the solubility of a two-component H_2O+CO_2 fluid in silicate liquids. *Am. Mineral.*, **84**, 477-492.

Papale, P., Moretti, R., Barbato, D. (2006): The compositional dependence of the saturation surface of H_2O + CO_2 fluids in silicate melts. *Chem. Geol.*, **229**, 78-95.

Robinson, B.W., Ware, N.G., Smith, D.G.W. (1998): Modern electron-microprobe trace-element analysis in mineralogy, *in* "Modern approches of the ore and environmental mineralogy", L.J. Cabri, D.J. Vaughan, eds. Mineralogical Association of Canada, Short-course, **27**, 153-180.

Scaillet, B. & Pichavant, M. (2003): Experimental constraints on volatile abundances in arc magmas and their implications for degassing processes, *in* "Volcanic degassing", C. Oppenheimer, P.D.M., J. Barclay eds. Geol. Soc. Spec. Publ., London, 213, 23-52.

—, — (2005): A model of sulphur solubility for hydrous mafic melts: application to the determination of magmatic fluid compositions of Italian volcanoes. *Ann. Geophys.*, **48**, 671-698.

Shinohara, H., Iiyama, J.T., Matsuo, S. (1989): Partition of chlorine compounds between silicate melt and hydrothermal solutions: I. Partition of NaCl-KCl. *Geochim. Cosmochim. Acta*, **53**, 2617-2630.

Shmulovich, K.I. & Graham, C.M. (1999): An experimental study of phase equilibria in the system H_2O-CO_2-NaCl at 800 °C and 9 kbar. *Contrib. Mineral. Petrol.*, **136**, 247-257.

—, — (2004): An experimental study of phase equilibria in the systems H_2O-CO_2-$CaCl_2$ and H_2O-CO_2-NaCl at high pressures and temperatures (500-800 °C, 0.5-0.9 GPa): geological and geophysical applications. *Contrib. Mineral. Petrol.*, **146**, 450-462.

Sisson, T.W. & Layne, G.D. (1993): H_2O in basalt and basaltic andesite glass inclusions from 4 subduction-related volcanos. *Earth Planet. Sci. Lett.*, 117, 619-635.

Symonds, R.B., Rose, W.I., Bluth, G.J.S., Gerlach, T.M. (1994): Volcanic-gas studies: Methods, results and applications, *in* "Rev. Mineral.", M.R. Carroll, J.R. Holloway, eds. Mineralogical Society of America, Washington, **30**, 1-66.

Tamic, N., Behrens, H., Holtz, F. (2001): The solubility of H_2O and CO_2 in rhyolitic melts in equilibrium with a mixed CO_2-H_2O fluid phase. *Chem. Geol.*, **174**, 333-347.

Taylor, J.R., Wall, V.J., Powneby, M.I. (1992): The calibration and application of accurate redox sensors. *Am. Mineral.*, **77**, 284-295.

Wallace, P.J. (2005): Volatiles in subduction zone magmas: concentrations and fluxes based on melt inclusion and volcanic gas data. *J. Volcanol. Geotherm. Res.*, **140**, 217-240.

Webster, J.D. & De Vivo, B. (2002): Experimental and modeled solubilities of chlorine in aluminosilicate melts, consequences of magma evolution, and implications for exsolution of hydrous chloride melt at Mt. Somma-Vesuvius. *Am. Mineral.*, **87**, 1046-1061.

Webster, J.D. & Holloway, J.R. (1988): Experimental constraints on the partitioning of Cl between topaz rhyolite melt and H_2O and H_2O + CO_2 fluids - New implications for granitic differentiation and ore deposition. *Geochim. Cosmochim. Acta*, **52**, 2091-2105.

Webster, J.D., Kinzler, R.J., Mathez, E.A. (1999): Chloride and water solubility in basalt and andesite melts and implications for magmatic degassing. *Geochim. Cosmochim. Acta*, **63**, 729-738.

Webster, J.D., Tappen, C., Sintoni, M.F., De Vivo, B. (2004): Experimentally determined H_2O, S, and Cl solubilities in phonolite melt at 200 MPa: Implications for volatile exsolution and eruption of Mt. Somma-Vesuvius magmas. *Eos Trans. AGU*, **85**, Jt. Assem. Suppl., Abstract V54B-03.

Received 28 December 2006
Modified version received 25 April 2007
Accepted 14 June 2007